J Wood Sci (2004) 50:391–399
DOI 10.1007/s10086-003-0606-y

ORIGINAL ARTICLE

Masahiro Noguchi · Kohei Komatsu

A new method for estimating stiffness and strength in bolted timber-to-timber joints and its verification by experiments (II): bolted cross-lapped beam to column joints

Received: March 20, 2003 / Accepted: October 8, 2003

Abstract Bolted cross-lapped joints (BCLJs) are one of the basic jointing methods used in Japan and European countries. There are, however, some problems in the design of BCLJs. With increasing use of large-scale wooden frame structures in Japan, it is necessary to establish proper estimating methods for predicting actual characteristics. A new approach was developed, using Saint Venant torsion theory, to estimate the performance of bolted timber joints in a more practical manner than using computer simulations. The calculated values were compared with the experimental results, indicating that the rotational stiffness and yield moment of BCLJs would be precisely predicted using the proposed theory. It was also found that the rotational stiffness calculated using the design method rooted on Coulomb's torsion theory is about two times higher than the experimental results in the case of a rectangular arrangement of bolts.

Key words Bolted cross-lapped joints · Torsion · Timber · Mechanical model

Introduction

Bolted cross-lapped joints (BCLJs) have been used as one of the basic jointing techniques in large-scale wooden frame structures. Some effective types of BCLJ were developed by Leijten,[1,2] Haller et al.,[3] Haller,[4] Leicti et al.,[5] Larsen,[6] and Rodd.[7] There are, however, some problems in the design methods of BCLJ.

Most designs are based on Coulomb's torsion theory, the same as the number of rivets of steel frame structures.[8,9] Coulomb's torsion theory is limited in two conditions: the twist of circular shafts of constant cross section, and torsion of a slice of the bar between two cross sections attached to rigid plate. To simplify, it is thought that the BCLJ can be divided into the three parts of joint layer, side member, and main member, as in Fig. 1.

In the case of the number of rivets in steel frame structures, it can, according to Goodier's hypothesis,[10] be assumed that the distribution of shear force of rivet is governed by Coulomb's law. It can be modelled as a slice of the joint layer between two cross sections attached to the rigid plate – joint layer assembly. Figure 2 shows the thickness can be assumed to be a slice, the angle at the arbitrary point through the longitudinal direction of rivet is constant, and the members made of steel can be assumed to be rigid bodies. On the other hand, it is questionable to apply Coulomb's law to BCLJ without a circular bolt arrangement. If BCLJ has a joint layer, the thickness of the BCLJ cannot be assumed to be a slice. The angles at the arbitrary point through the longitudinal direction of rivet are different, and members made of timber cannot be assumed to be rigid bodies, as in Fig. 3.

Ohashi and Sakamoto[11] pointed out that timber members could not be assumed to be a rigid bodies, but should, perhaps, be assumed to be elastic bodies. Ono et al.[12] also pointed out that the bolts of the BCLJ may not work as supposed in conventional theories[8,9] without the circular arrangement of bolts.

To promote the use of large-scale wooden frame structures in Japan and other countries, it is important to predict their actual characteristics correctly. In this study, a manual design method is developed in terms of yield strength and rotational stiffness of BCLJs by considering timber deformation, and not using Coulomb's law, but rather using Saint Venant torsion theory.

Theory

For BCLJs, it had been recognized that beams or columns transmit bending moment at the panel zone, as in Fig. 4. Therefore, it can be reasonably assumed that each member

M. Noguchi (✉) · K. Komatsu
Research Institute for Sustainable Humanosphere, Kyoto University, Uji 611-0011, Japan
Tel. +81-774-38-3670; Fax +81-774-38-3678
e-mail: noguchan@rish.kyoto-u.ac.jp

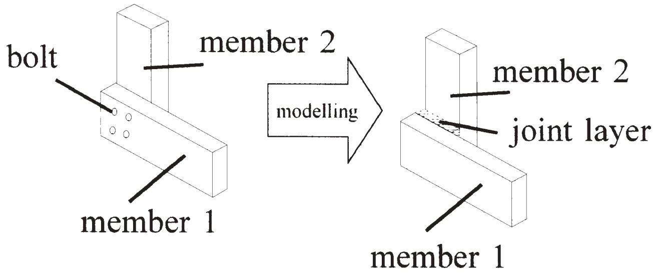

Fig. 1. Modelling of bolted cross-lapped joints (BCLJ)

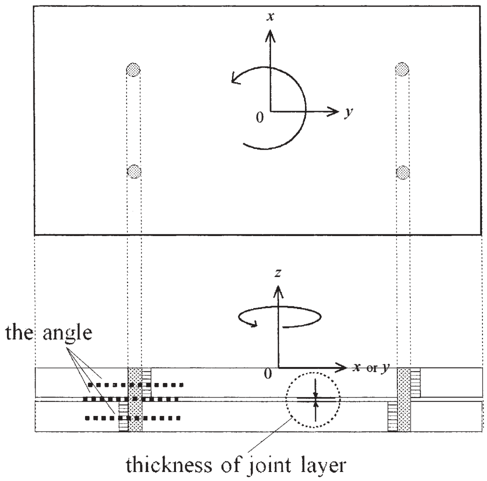

Fig. 2. Model of number of rivets of steel frame structures

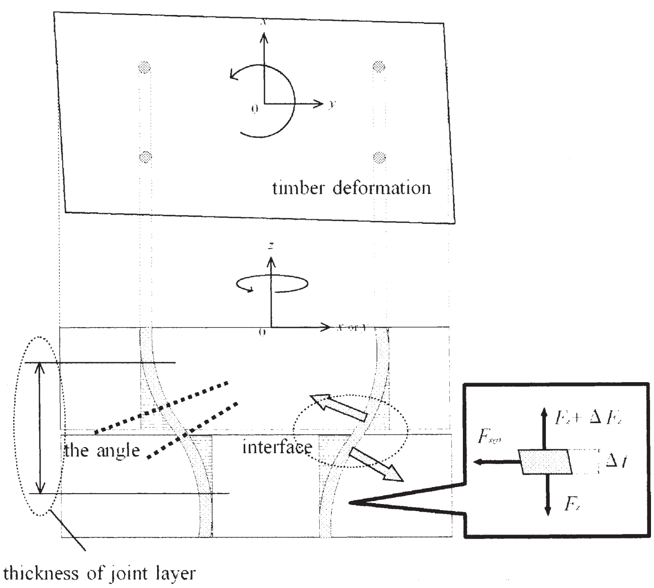

Fig. 3. Model of BCLJ

is subjected to a bending moment M, and a coupling moment M, which forms a torque M to resist the bending deformation of bolts. The joint layer, assuming bolts as a joint layer, is twisted by the torque M. It can be thought that BCLJ has three deformation factors: shear deformation of timber, bending deformation of timber, and bending deformation of bolts, as in Fig. 5. Shear forces of bolts are actually complicated mechanisms that consist of member deformation at the panel zone, and bending deformation of the bolt, as in Fig. 6. To derive a simple design method, the following hypotheses are set:

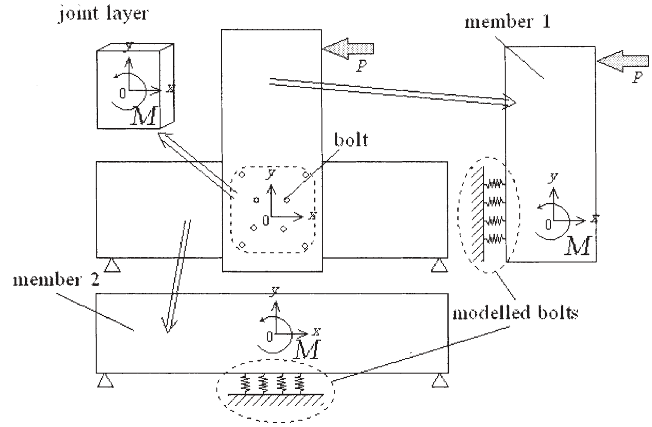

Fig. 4. Concept for a mechanical model of a BCLJ

BCLJ can be divided into the three parts of joint layer, side member, and main member, as shown in Figs. 1 and 2.

P_i would be composed to the shear force of bolts ($P_{\mathrm{RB}i}$) due to joint layer, and the shear force of bolt ($P_{j\mathrm{TB}i}$) due to the member deformation at panel zone, as in Fig. 6.

The shear force of the bolts is decomposed to the shear force due to shear force and the applied shear force due to moment.

Joint layer

There are two theories on static torsion, shown in Fig. 7. The stress distributions, according to Coulomb's law,[10] are in proportion to the distances from the rotational centers. The stress distributions, according to Saint Venant's torsion theory,[13] are not in proportion to the distances from the rotational center. The stress distributions of shorter sides are larger than those of longer sides, as shown in Fig. 7.

In this study, Saint Venant's torsion theory is considered, because BCLJ that have slender bolts cannot meet Goodier's hypothesis, i.e., the panel zone is assumed to be a rigid body, or bolts do not have the required length. There are still some problems in using Saint Venant's torsion theory to derive a practical design equation. For example, this theory cannot be calculated without a computer. In addition, it is impossible to explain the load distribution of bolts using this theory, because the mechanisms of BCLJ are not real torsions. Saint Venant's torsion theory is a target for a continuum. A boundary condition must be satisfied at the surface, i.e., normal stress is equal to zero at the surface, as in Fig. 8a. This boundary condition outlines the character of the stress distribution. The highest stress is found at the middle of the sides, and the lowest stress is found at the corner of the sides, as in Fig. 7. In the case of

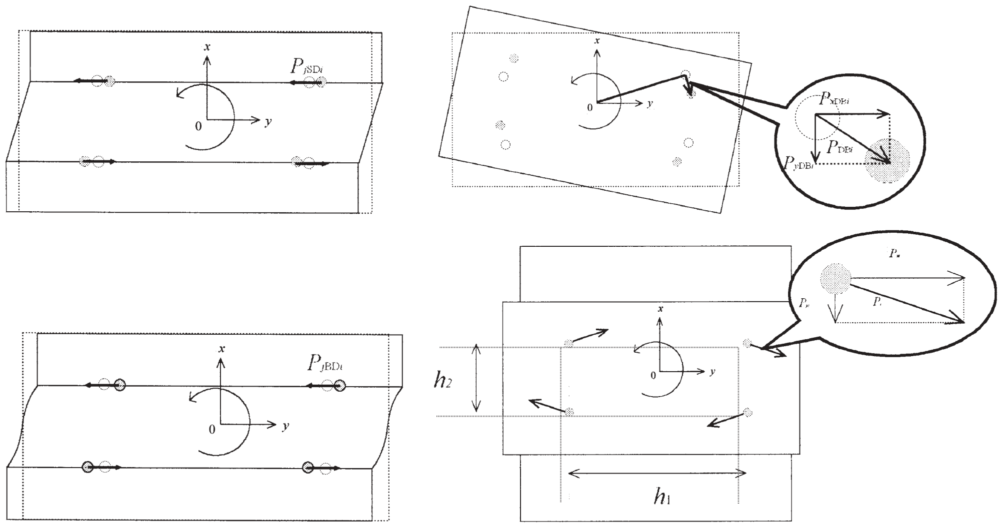

Fig. 5. Shear force of bolts: various factors at interface between member 1 and member 2

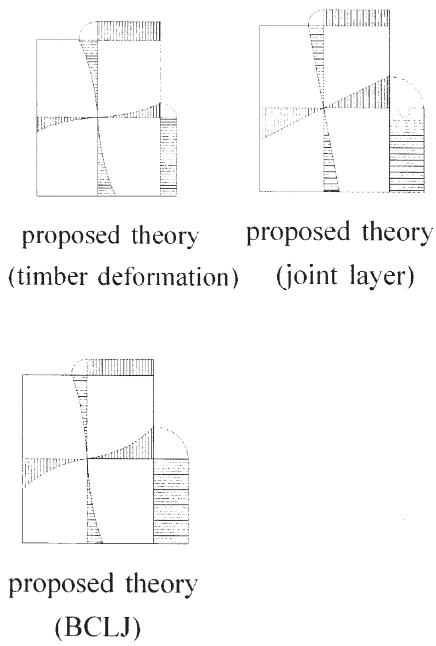

Fig. 6. Distribution of shear force of a BCLJ based on proposed theory

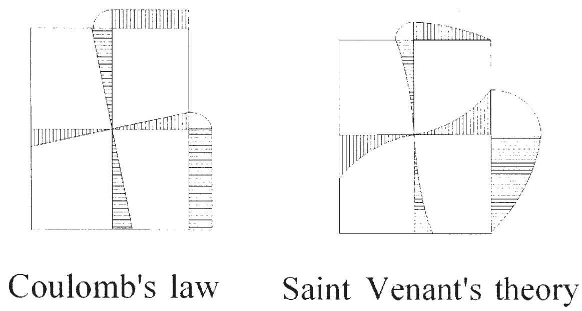

Fig. 7. Distribution of shearing stress according to Coulomb's law and Saint Venant's torsion theory

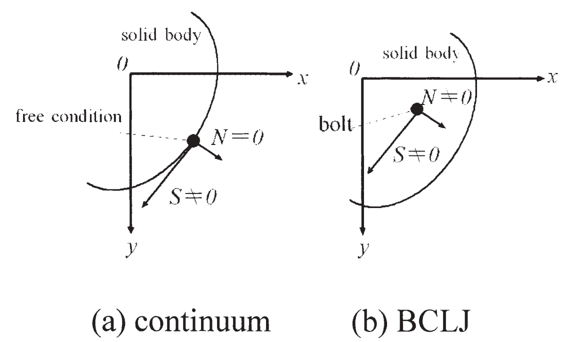

Fig. 8. Boundary condition

BCLJ, normal stress is zero at the outermost bolts. Therefore, it is assumed that the distribution of x and y components of shear forces are constant at the same distance from the y- and x-axes. The distribution of the x and y components of shear force is proportional to the distance from the y- and x-axes, as shown in Fig. 6. The following relationships exist:

$$P_{xRBi} = \beta_x x_i \qquad \beta_x\text{: undetermined coefficient} \tag{1}$$

$$P_{yRBi} = \beta_y y_i \qquad \beta_y\text{: undetermined coefficient} \tag{2}$$

The relationship between β_x and β_y is determined by Saint Venant torsion theory. In the case of Coulomb's law, β_x and β_y are the same value, or are determined by geometry. According to Timosienko and Goodier,[13] it was found that half the torque was due to the x-components of the shearing stress and the other half to the y-components in Saint Venant torsion theory. In this study, it can also be assumed that the moment due to x-components of shear forces is equal to that due to y-components.

$$M_{tx} = \frac{1}{2}M, M_{ty} = \frac{1}{2}M \tag{3}$$

Timber deformation

Bending moment M causes two deformations on each member, i.e., shear deformation of timber and bending deformation of timber. Assuming that shearing stress distribution of timber at the panel zone is a constant, and $P_{j\mathrm{SD}i}$ is also proportional to the distance from the y-axis, as in Fig. 5.

$$P_{j\mathrm{SD}i} = \gamma_j x_i \qquad \gamma_j\text{: undetermined coefficient} \tag{4}$$

Considering timber bending deformation at the panel zone, shear stress distribution of timber at the panel zone by M can be assumed to be a constant. Each member is considered as a beam. Using basic beam theory, the following relationship exists:

$$Q_{jM} = \frac{M}{h_j} = \frac{d^3\delta_j(x_i)}{dx_i^3} \qquad \text{where, } h_j\text{: depth of timber } j \tag{5}$$

Meanwhile, the center of bolt arrangement is thought to be symmetrical, and the following boundary conditions are possible:

$$M_j(0) = 0, \delta_j(0) = 0, \text{ and } \theta_j(0) = 0. \tag{6}$$

Using these boundary conditions and Eq. 5, $\delta_j(x_i)$ can be derived as follows:

$$\delta_j(x_i) = \frac{Mx_i^3}{6h_jE_jI_j} \tag{7}$$

The load distribution of a bolt due to timber bending at the panel zone is expressed as the product of the bending deformation of timber $\delta_j(x_i)$ and the semi slip modulus[16] K_{h90ji} of a bolt perpendicular to the grain. From the above, the load distribution $P_{j\mathrm{TB}i}$ of a bolt by bending deformation of timber has the following form:

$$P_{j\mathrm{TB}i} = \delta_j(x_i) \times K_{h90ji} = \frac{MK_{h90ji}x_i^3}{6h_jE_jI_j} \tag{8}$$

Corresponding to the x-component, the shear force of bolt P_{xMi} can be expressed as follows:

$$P_{xMi} = P_{j\mathrm{TB}i} + P_{j\mathrm{RB}i} + P_{j\mathrm{SD}i} \tag{9}$$

To simplify, a new parameter α is employed;

$$\alpha = \beta_x + \gamma_j \qquad \alpha\text{: undetermined coefficient} \tag{10}$$

P_{ix} can be expressed as follows:

$$P_{xMi} = \alpha x_i + \frac{MK_{h90ji}x_i^3}{6h_1E_1I_1} \tag{11}$$

Moment due to x-component must be satisfied:

$$M = \sum_{i=1}^{n} P_{xMi}x_i \tag{12}$$

From Eqs. 11 and 12, by eliminating α, P_{xMi} is obtained:

$$P_{xMi} = \frac{Mx_i}{\sum_{i=1}^{n} x_i^2} + \frac{K_{h90ji}M}{6E_1I_1h_1}\left(x_i^3 - \frac{x_i\sum_{i=1}^{n} x_i^4}{\sum_{i=1}^{n} x_i^2}\right) \tag{13}$$

and P_{yMi} can be obtained in the same way as P_{xMi}:

$$P_{yMi} = \frac{My_i}{\sum_{i=1}^{n} y_i^2} + \frac{K_{h90ji}M}{6E_2I_2h_2}\left(y_i^3 - \frac{y_i\sum_{i=1}^{n} y_i^4}{\sum_{i=1}^{n} y_i^2}\right) \tag{14}$$

Here, applied shear force P is assumed to be distributed to each bolt uniformly, i.e.:

$$P_{si} = \frac{P}{n} \tag{15}$$

The total bolt load, therefore, contains P_{si} and P_{xMi}.

From the above, P_{ix} and P_{iy} are expressed as:

$$P_{ix} = P_{xMi} + \frac{M\varphi}{n} \tag{16}$$

$$P_{iy} = P_{yMi} + \frac{M\psi}{n} \tag{17}$$

where, $\phi = P/M$, $\Psi = P/M$.

As the component of shear force due to the coupling moment is composed torsion moment, it can be thought that the resultant force P_i consists of P_{ix} and P_{iy} is the shear force of arbitrary bolt at interface between member 1 and member 2, as in Fig. 5a. The resultant force P_i can, therefore, be simply calculated as:

$$P_i = \sqrt{P_{ix}^2 + P_{iy}^2} \tag{18}$$

From above, the equation for yield moment of BCLJ (M_y) is obtained as:

$$M_y = \min(M_{yi})$$

where

$$M_{yi} = \frac{P_{yi}}{\sqrt{x_i^2 + y_i^2}} \tag{19}$$

$$X_i = \frac{x_i}{\sum_{i=1}^{n} x_i^2} + \frac{K_{h90ji}}{6E_1I_1h_1}\left(x_i^3 - \frac{x_i\sum_{i=1}^{n} x_i^4}{\sum_{i=1}^{n} x_i^2}\right) + \frac{\varphi}{n}$$

$$Y_i = \frac{y_i}{\sum_{i=1}^{n} y_i^2} + \frac{K_{h90ji}}{6E_2I_2b_2}\left(y_i^3 - \frac{y_i\sum_{i=1}^{n} y_i^4}{\sum_{i=1}^{n} y_i^2}\right) + \frac{\psi}{n}$$

Estimation of rotational stiffness of BCLJ will be derived as follows.

Total energy U at joint part is:

$$U = \frac{1}{2}\sum_{i=1}^{n} P_iS_i + \frac{1}{2}\int_0^{h_j}\frac{M^2}{E_jI_j}dxdy + \frac{1}{2}\int_0^{h_j}Q_{jM}\gamma_{sj}dxdy \tag{20}$$

Castigliano's first theorem is expressed in Eq. 21:

$$\theta = \frac{\vartheta U}{\vartheta M} \tag{21}$$

From Eqs. 20, 21 and basic beam theory, the rotational stiffness of BCLJ (R) is as follows:

$$R = \frac{1}{\sum_{i=1}^{n}\left(\frac{P_{xMi}^2 + P_{yMi}^2}{K_{si}}\right) + \frac{1}{G_1 b_1 t_1 h_1} + \frac{1}{G_2 b_2 t_2 h_2} + \frac{h_1^2}{48EI} + \frac{h_2}{48E_2 I_2}} \tag{22}$$

In the case of ignorance of timber deformation, Eq. 19 can be expanded as:

$$M_y = \min\left(M_{yi}\right)$$

where

$$M_{yi} = \frac{P_{yi}}{\sqrt{\frac{x_i^2}{4\left(\sum_{i=1}^{n} x_i^2\right)^2} + \frac{y_i^2}{4\left(\sum_{i=1}^{n} y_i^2\right)^2}}} \tag{23}$$

In the case of ignorance of timber deformation, Eq. 22 can be simplified as:

$$R = \frac{4}{\frac{\sum_{i=1}^{n}\frac{x_i^2}{K_{si}}}{\left(\sum_{i=1}^{n} x_i^2\right)^2} + \frac{\sum_{i=1}^{n}\frac{y_i^2}{K_{si}}}{\left(\sum_{i=1}^{n} y_i^2\right)^2}} \tag{24}$$

In the case of cross-grained members, K_{si} would be assumed as a constant value K_s.[8,9] Thus, Eq. 24 can be simplified as:

$$R = \frac{4K_s \sum_{i=1}^{n} x_i^2 \sum_{i=1}^{n} y_i^2}{\sum_{i=1}^{n} x_i^2 + \sum_{i=1}^{n} y_i^2} \tag{25}$$

Materials and methods

Specimens

Figure 9 shows BCLJ specimens used in this study. Each BCLJ specimen consists of a column (160 × 500 × 1500 mm) and a pair of beams (80 × 500 × 2000 mm). They were joined with bolts and formed a T-shaped assembly. Bolts were arranged in a rectangle or square with the number of bolts ranging from 4 to 16, see Fig. 10. Each bolt had a diameter of 16 mm, and a length of 32 mm. Clearance between the bolt and the predrilled hole was 1 mm in all specimens. Columns and beams were made of Douglas-fir glulam having JAS grade of E105 – f 300, with an average moisture content of 11%, and mean density of 456 kg/m^3.

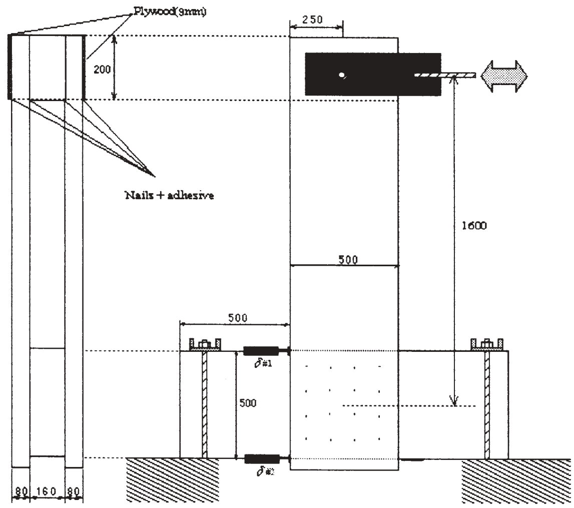

Fig. 9. Specimen dimensions (mm) and experimental setup

Cyclic load[14] was applied, as in Fig. 9. Moment (M) and rotational angle of BCLJ (θ) are defined as follows:

$$M = 1.85(\mathrm{m}) \times P \tag{26}$$

$$\theta = \frac{\delta_{\#1} - \delta_{\#2}}{500} \tag{27}$$

where P is applied load (kN), and $\delta_{\#1}$ and $\delta_{\#2}$ are relative displacement (mm), shown in Fig. 9.

Results and discussion

Verification

Material properties for numerical calculation were adopted from previous studies,[15,16] except for the bearing properties of bolts. The bearing property was calculated using the modulus of elasticity of the laminas. The slip modulus and the yield strength of single bolted joints were calculated using the proposed equation,[17] as follows:

Slip modulus

$$K_{si} = \frac{K_{h1i}}{K_{h1i}} + \frac{K_{h2i}}{K_{h2i}} \tag{28}$$

Where;

$$K_{hji} = \frac{2\lambda_{ji}^3 (EI)_s \left(\sinh \gamma_{ji} t_{ji} \cosh \lambda_{ji} t_{ji} + \sin \lambda_{ji} t_{ji} \cos \lambda_{ji} t_{ji}\right)}{\cosh^2 \lambda_{ji} t_{ji} - \sin^2 \lambda_{ji} t_{ji}}$$

Table 1. Definitions of symbols

Symbol	Definition
b_j	Width of member *j*
d_i	Diameter of *i*-th bolt
E_j	Modulus of elasticity in member *j*
EI_{si}	Bending stiffness of *i*-th bolt
G_j	Shear modulus of member *j*
h_j	Length of member *j*
i	*i*-th bolt
I_j	Moment of inertia of member *j*
j	1 is main member, 2 is side member
K_{h90ij}	Semi slip modulus of *i*-th bolt perpendicular to the grain in member *j*
K_{hji}	Semi slip modulus of the *i*-th bolt in member *j*
k_{ji}	Bearing constant of *i*-th bolt in member *j*
K_{si}	Slip modulus of the *i*-th bolt
K_s	Slip modulus
M	Working moment at panel zone
$M_j(x)$	The function of moment distribution in member *j*
M_{tx}	*x*-component of *M*
M_{ty}	*y*-component of *M*
M_v	Yield moment of BCLJ
M_{vi}	Yield moment calculated by *i*-th bolt
n	The number of bolt in BCLJ
P	Applied load
P_{hbji}	Yield strength calculated assuming bolt bending yield of *i*-th bolt in member *j*
P_{hwji}	Yield strength calculated assuming wood bearing yield of *i*-th bolt in member *j*
P_{hvji}	Yield strength of *i*-th bolt in member *j*
P_i	Shear force of *i*-th bolt
P_{ix}	*x*-component of shear force of *i*-th bolt
P_{iy}	*y*-component of shear force of *i*-th bolt
P_{ji}	Shear force of *i*-th bolt due to both coupling moment and shear force in member *j*
P_{xMi}	The component of shear force of *i*-th bolt due to moment in member *j*
P_{yMi}	The component of shear force of *i*-th bolt due to moment in member *j*
P_{RBi}	Shear force of *i*-th bolt due to torsion of joint layer
P_{xRBi}	*x*-component of shear force of *i*-th bolt due to torsion of joint layer
P_{yRBi}	*y*-component of shear force of *i*-th bolt due to torsion of joint layer
P_{jSDi}	Shear force of *i*-th bolt due to timber shear deformation at panel zone of in member *j*
P_{si}	Shear force of *i*-th bolt due to applied shear force
P_{jTBi}	Shear force of *i*-th bolt due to timber bending deformation at panel zone in member *j*
P_{vj}	Yield strength of *i*-th bolt in member *j*
R	The rotational stiffness of BCLJ
r_i	Distance between the centre of bolt arrangement and *i*-th bolt
S_i	The slip of *i*-th bolt
t_{ji}	Length of the *i*-th bolt in member *j*
U	Total energy at joint part
x_i	The distance from *x*-axis in *i*-th bolt
y_i	The distance from *y*-axis in *i*-th bolt
Z	Section modulus
α	Undetermined coefficient
β_x	Undetermined coefficient
β_y	Undetermined coefficient
γ_j	Undetermined coefficient in member *j*
γ_{sj}	Shear strain of member *j*
$\delta_{\#1}$	Relative displacement between timber and beam in experimental work in Fig. 9
$\delta_{\#2}$	Relative displacement between timber and beam in experimental work in Fig. 9
$\delta_j(x)$	The function of bending deformation of timber at x in member j
θ	Rotational angle of BCLJ
$\theta_j(x)$	The function of the angle of beam at in member *j*
λ_{ji}	Coefficient of *i*-th bolt in member *j*
σ_{syi}	Yield stress of steel in *i*-th bolt
σ_{yji}	Bearing yield stress of *i*-th bolt in member *j*
Qj_M	The average shear stress of member at panel zone due to moment worked at panel zone in member *j*
φ	Coefficient
Ψ	Coefficient

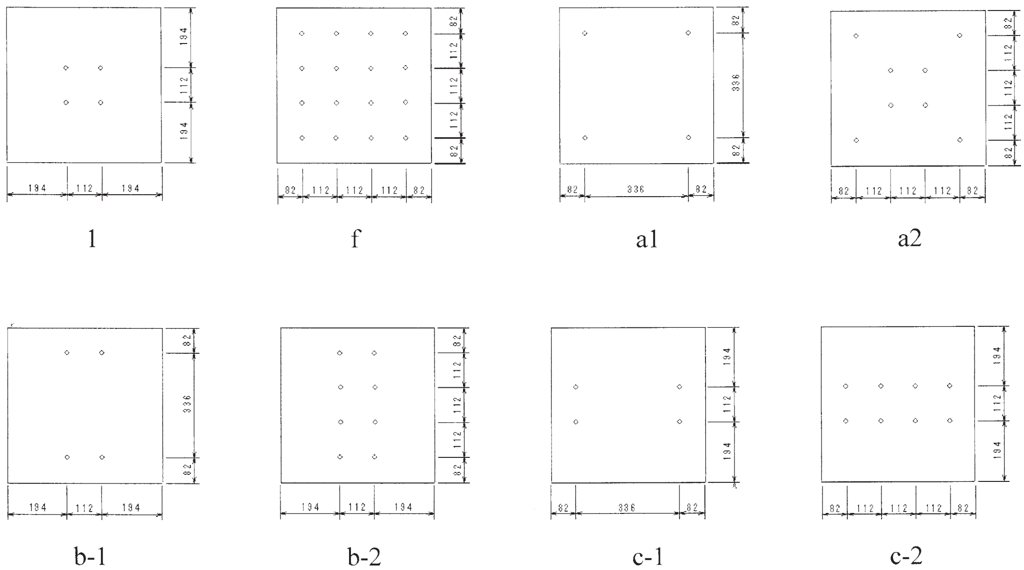

Fig. 10. Bolt arrangements of specimens (unit: mm)

$$\lambda_{ji} = \sqrt[4]{\frac{k_{ji} d_i}{4(EI)_{si}}}$$

Yield strength

$$P_{yi} = \min\left\{P_{hy1i} \text{ in maim member}, P_{hy2i} \text{ in side member}\right\} \quad (29)$$

Where;

$$P_{hy} = \min\left\{P_{hwji}, P_{hbji}\right\}$$

$$P_{hbji} = \frac{k_{ji}\sigma_{syi} Z_i d_i}{0.6K_{hji}} \quad P_{hwji} = \frac{K_{hji}\sigma_{yij}}{k_{ji}}$$

$$Z_i = \frac{d_{ji}^3}{6}$$

The comparisons between theoretical calculations and experimental results, shown in Fig. 11, shows that rotational stiffness and the yield moment of BCLJ can be precisely predicted by using the proposed theory without type 1. In the case of specimen 1, the practical values of yield moment and rotational stiffness are lower than the calculated values. It was considered that only a few bolts worked, because the distance between the bolt and rotational shaft in specimen 1 was much smaller than that of the other specimens. The influence of clearance is governed by the distance between the bolt and rotational shaft. Therefore, the mechanism of specimen 1 is different from the supposed mechanism of the proposed theory.

For rotational stiffness, the estimated values by conventional theory[4] are about two times higher than the experimental results for the rectangular bolt arrangement, as in Fig. 11. The difference of values between conventional theory and experimental data is not thought to be a result of the clearance between the bolts and the predrilled holes, but due to shortcoming of Saint Venant's torsion theory. If the clearance does have any influence, such a difference should also exist in the case of the square bolt arrangement.[18,19]

Relationship between proposed theory and conventional theory

In the case of symmetrical arrangement of bolts on both the x-axis and y-axis, Eq. 30 remains consistent, i.e.:

$$\sum_{i=1}^{n} x_i^2 = \sum_{i=1}^{n} y_i^2 \quad (30)$$

Therefore, Eq. 25 can be simplified as:

$$R = 2K_s \sum_{i=1}^{n} x_i^2 \quad (31)$$

Using Eq. 30, conventional theory can be expressed as:

$$R = \sum_{i=1}^{n} K_{s_i} r_i^2 \quad (32)$$

where;

$$r_i^2 = x_i^2 + y_i^2$$

In the case of a symmetrical arrangement of bolts on both the x-axis and y-axis, Eq. 32 can be simplified as:

$$R = 2K_s \sum_{i=1}^{n} x_i^2 \quad (33)$$

Equation 31 is the same as Eq. 33. From this, in the case of symmetrical arrangement of bolts on both the x-axis and y-

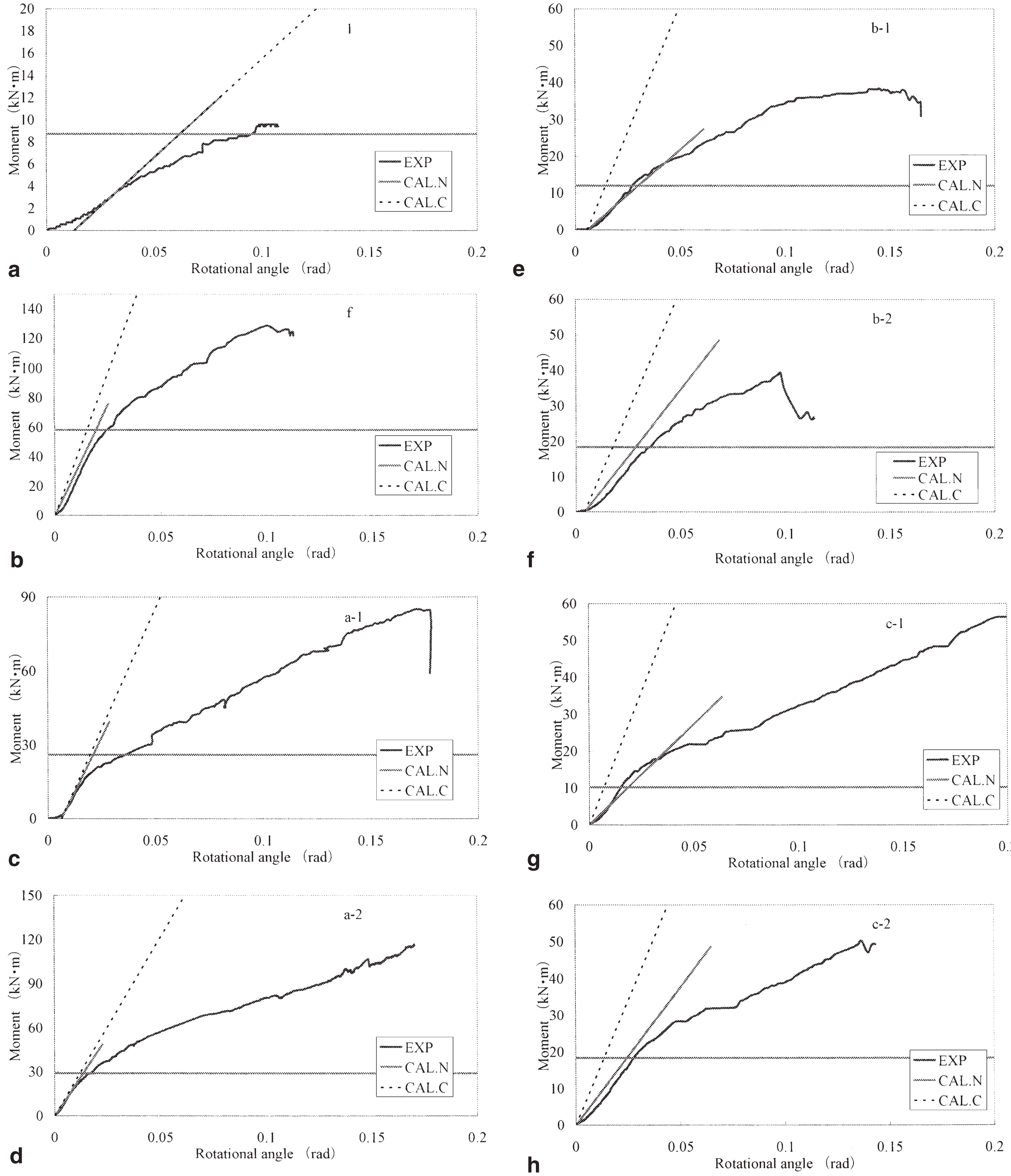

Fig. 11a–h. Comparison between experimental results and estimated values using proposed theory in BCLJs for different bolt arrangements. *EXP*, experimental result; *CAL.C*, rotational stiffness calculated by conventional theory, Eq. 32; *CAL.N*, rotational stiffness and yield moment calculated by our proposed theory, Eqs. 22 and 19

axis, rotational stiffness determined from the proposed theory has the same value as that from conventional theories.

Conclusions

A new approach was developed to estimate the performance of bolted timber joints in a practical manner, rather than based on computer simulation. From the theoretical and experimental results, it can be concluded that the rotational stiffness and yield moment in bolted cross-lapped joints can be precisely predicted by the proposed theory. In the case of rectangular bolt arrangement, the rotational stiffness calculated using conventional theory was about two times higher than the experimental results. Therefore, it is not reasonable to use the theory rooted to Coulumb's law for estimating rotational stiffness in the case of a rectangular arrangement of bolts.

Acknowledgments The authors thank Dr. Meng Gong for his kind assistance in reviewing the draft.

References

1. Leijten AJM (1998) Reinforced joints with expanded tube fasteners. In: Densified veneer wood reinforced timber joints with expanded tube fasteners. Delft University Press, Delft, pp 57–96
2. Leijten AJM (1988) Steel reinforced joints with dowels and bolts. In: Proceedings of International Conference on Timber Engineering, Washington, vol 2, pp 475–488
3. Haller P, Chen CJ, Natterer J (1996) Experimental study on glass fibre reinforced and densified timber. In: Proceedings of International Wood Engineering Conference, New Orleans, USA, vol 1, pp 308–314
4. Haller P (1999) Semi-rigid timber joints – structural behaviour, modelling and new technologies. Final Report of Working Group on Timber Joints
5. Leichti RJ, Tjahyadi A, Bienhaus A, Gupta R, Miller T, Duff S (2002) Design and behaviour of frictio dampers for two-dimensional braced and moment-resisting timber frames. In: Proceedings of World Conference on Timber Engineering, Shah Alam, Malaysia, vol 2, pp 267–274
6. Larsen HJ (1996) Glass fibre reinforcement of dowel-type joints. In: Proceedings of International Wood Engineering Conference, New Orleans, USA, pp 293–302
7. Rodd PD (1996) Resin injected dowels in moment transmitting joints. In: Proceedings of International Wood Engineering Conference, New Orleans, USA, pp 169–176
8. Racher P (1995) Moment resisting connections In: Timber engineering STEP 1. Centrum Hout, Almere, pp C16/1–C16/11
9. Isoda H (1996) Design method of portal frame using GLT (in Japanese). Tokyo, pp 35–46
10. Goodier JN (1942) An extension of Saint-Venant's Principle with applications. J Appl Phys 3:167–171
11. Ohashi Y, Sakamoto I (1989) Study on laminated timber moment resisting joint. In: Proceedings of the Second Pacific Timber Engineering Conference, Auckland, New Zealand, vol 2, pp 37–42
12. Ono T, Ando K, Itoda H, Kato Y (2001) Study on stiffness and ultimate strengths of drift-pin joints of glue-laminated wood members (in Japanese). J Struct Constr Eng 536:101–106
13. Timoshenko S, Goodier JN (1951) Torsion. In: Theory of elasticity. Kogakuaha, Tokyo, pp 258–263
14. The Building Center of Japan (2002) The building letter. 443:27–32
15. Komatsu K, Karube M, Harada M, Fukuda I, Hara Y, Kaihara H (1996) Strength and ductility of glulam portal frame designed by considering yield of fasteners in part. In: Proceedings of International Wood Engineering Conference, New Orleans, USA, pp 523–529
16. Architectural Institute of Japan (AIJ) (1995) Moment resisting joints (in Japanese). In: Structural design note for timber structures. Maruzen, Tokyo, pp 184–221
17. Noguchi M, Komatsu K (2003) New proposal for estimating method of stiffness and strength in the bolted timber-to-timber joints and its verification by experiments (in Japanese). Mokuzai Gakkaishi 49:92–103
18. Tsuchimoto T (2002) Stochastic estimation of deflection properties on portal frames jointed by bolts with initial clearance. In: Proceedings of World Conference on Timber Engineering, Shah Alam, Malaysia, vol 2, pp 485–493
19. Tsuchimoto T, Ando M, Arima T, Suzuki T (1999) Effect of clearance on the mechanical properties of timber joint. In: Proceedings of Pacific Timber Engineering Conference, Rotorua, New Zealand, vol 2, pp 204–210